David J. Yang, PhD
Chang-Guhn Kim, MD
Naomi R. Schechter, MD
Ali Azhdarinia, MS
Dong-Fang Yu, MS
Chang-Sok Oh, PhD
Jerry L. Bryant, MS
Jong-Jin Won, MD
E. Edmund Kim, MD
Donald A. Podoloff, MD

Index terms:
Contrast media, experimental studies
Experimental study
Neoplasms, experimental studies
Radionuclide imaging, experimental studies

Published online before print
10.1148/radiol.2262011811
Radiology 2003; 226:465–473

Abbreviations:
ECDG = ethylenedicysteine–deoxyglucose
FDG = fluorodeoxyglucose
ROI = region of interest

[1] From the Divisions of Diagnostic Imaging (D.J.Y., C.G.K., A.A., D.F.Y., C.S.O., J.L.B., J.J.W., E.E.K., D.A.P.) and Radiation Oncology (N.R.S.), University of Texas M.D. Anderson Cancer Center, 1515 Holcombe Blvd, Houston, TX 77030. From the 2001 RSNA scientific assembly. Received November 9, 2001; revision requested January 7, 2002; final revision received May 16; accepted June 18. The animal research and nuclear magnetic resonance facility used in this study was supported by M.D. Anderson Cancer Center (Cancer Center Support Grant) grant NIH CA-16672. Supported in part by Cell Point Research Fund. **Address correspondence to** D.J.Y. (e-mail: *dyang@di.mdacc.tmc.edu*).

Author contributions:
Guarantor of integrity of entire study, D.J.Y.; study concepts, E.E.K., N.R.S.; study design, D.J.Y., D.F.Y., E.E.K.; literature research, J.J.W., J.L.B.; clinical studies, E.E.K., C.G.K., D.A.P.; experimental studies, A.A., D.F.Y.; data acquisition, A.A., C.S.O.; data analysis/interpretation, A.A., J.L.B.; statistical analysis, A.A.; manuscript preparation, D.J.Y.; manuscript definition of intellectual content, D.J.Y., E.E.K., D.F.Y.; manuscript editing, D.A.P., E.E.K., C.G.K.; manuscript revision/review, E.E.K., D.J.Y.; manuscript final version approval, D.J.Y.

Imaging with ^{99m}Tc ECDG Targeted at the Multifunctional Glucose Transport System: Feasibility Study with Rodents[1]

PURPOSE: To evaluate the feasibility of technetium 99m (^{99m}Tc) ethylenedicysteine–deoxyglucose (ECDG) imaging in tumor-bearing rodents.

MATERIALS AND METHODS: ECDG was synthesized by means of reacting ethylenedicysteine with glucosamine, with carbodiimide as the coupling agent. Hexokinase assays were performed at an ultraviolet wavelength of 340 nm. To determine whether blood glucose level could be altered, ECDG or glucosamine was injected into six rats. In a separate study, ECDG followed by insulin was administered to three rats. To determine biodistribution, lung tumor cells were intramuscularly injected into the hind legs of 18 nude mice. The animals were then injected with ^{99m}Tc ECDG or fluorine 18 (^{18}F) fluorodeoxyglucose (FDG) (0.037–0.074 MBq per mouse). Radioactivity was measured in tissue excised from the animals. Scintigraphy was performed in three groups: in group 1 to demonstrate that different-sized tumors could be imaged after ^{99m}Tc ECDG administration, in group 2 to ascertain whether tumor uptake of ^{99m}Tc ECDG was perfusion related, and in group 3 to demonstrate that tumor uptake of ^{99m}Tc ECDG occurred by means of a glucose-mediated process.

RESULTS: ECDG was positive for phosphorylation at hexokinase assay. Blood glucose level increased with ECDG injection and decreased with insulin administration. Tumor-to–brain tissue and tumor-to–muscle tissue ratios of ^{99m}Tc ECDG uptake were higher than those of ^{18}F FDG uptake. Scintigraphic results demonstrated the feasibility of ^{99m}Tc ECDG imaging.

CONCLUSION: There are similarities between ^{99m}Tc ECDG uptake and ^{18}F FDG uptake in tumors, and study findings supported the potential use of ^{99m}Tc ECDG as a functional imaging agent.

Improvements in tumor scintigraphy are fundamentally dependent on the development of more tumor-specific radiopharmaceutical agents. Owing to greater tumor specificity, radiolabeled ligands and radiolabeled antibodies have led to a new era in the scintigraphic detection of tumors and undergone extensive preclinical development and evaluation. Radionuclide imaging modalities such as positron emission tomography (PET) and single photon emission computed tomography (CT) are diagnostic cross-sectional imaging techniques that enable one to map the location and concentration of radionuclide-labeled compounds (1–3). Although CT and magnetic resonance (MR) imaging yield considerable anatomic information about the location and extent of tumors, these modalities do not enable one to adequately differentiate residual or recurrent tumors from edema, radiation necrosis, or gliosis. PET and single photon emission CT can be used to localize and characterize active tumors by enabling measurement of metabolic activity.

Fluorine 18 (^{18}F) fluorodeoxyglucose (FDG) has been used to diagnose and stage tumors (4–14), myocardial infarction (15), and neurologic disease (16,17). Although tumor met-

abolic imaging with ^{18}F FDG has been studied for more than 2 decades, the use of this examination in clinical practice is still limited by factors such as difficult access, limited availability, and high cost (18). In addition, PET radiosynthesis must be performed rapidly because of the short half-life of the positron isotopes. ^{18}F chemistry studies are usually complicated and involve longer synthesis time (eg, 1 hour with FDG). Thus, it would be desirable to develop a simple technique to label agents with less costly isotopes for tissue-specific targeted imaging.

Technetium 99m (^{99m}Tc) has been preferred for labeling radiopharmaceutical agents owing to the low energy (140 Kev vs 511 Kev with ^{18}F) and inexpensive isotope cost ($0.21/MBq vs $50/MBq for ^{18}F) associated with the use of this element. Several ^{99m}Tc-labeled agents have been reported on; these include N_4 (eg, tetraazacyclododecane tetraacetic acid), N_3S (eg, mercapto acetyl triglycine), N_2S_2 (eg, ethylenedicysteine diethylester), NS_3,S_4 (eg, sulfur colloid), O_4 (eg, diethylenetriaminepentaacetic acid), and hydrazinenicotinamide chelates (19–24).

Diethylenetriaminepentaacetic acid does not chelate with ^{99m}Tc with stability that is comparable to that when it chelates with indium 111, however. Imaging with ^{99m}Tc-labeled hydrazinenicotinamide requires two additional chemicals, tricine and triphenylphosphine, to form a ^{99m}Tc complex and thus is inconvenient and costly. The nitrogen and sulfur combination, however, has been shown to be a stable chelate for ^{99m}Tc. In addition, bisaminoethanethiol tetradentate ligands, which are also known as diaminodithiol compounds, are known to form very stable technetium (valent V) oxide complexes owing to efficient binding of the oxotechnetium group to two thiolsulfur and two amine nitrogen atoms. ^{99m}Tc ethylenedicysteine is the most recent and successfully used N_2S_2 chelate (25,26). Ethylenedicysteine can be labeled with ^{99m}Tc easily, efficiently, and with high radiochemical purity and stability.

We previously reported on a series of ^{99m}Tc ethylenedicysteine conjugates for use in functional imaging in oncology (27–30). We hypothesize that ^{99m}Tc ethylenedicysteine–deoxyglucose (ECDG) is a specific multifunctional glucose transport–targeted agent. If the binding of ^{99m}Tc ECDG to tumor cells could be detected at planar scintigraphy or single photon emission CT, this depiction capability would suggest that the degree of malignancy (eg, tumor stage or tumor burden) of tumor cells could be imaged. Thus, the purpose of our study was to evaluate the feasibility of ^{99m}Tc ECDG imaging in tumor-bearing rodents.

MATERIALS AND METHODS

Chemicals and Analysis

Mass spectral analyses were conducted at the University of Texas Health Science Center in Houston, Texas. Nuclear MR spectra were recorded on a spectrometer (Bruker 500; Bruker Biospin, Rheinstetten, Germany). The mass data were obtained by means of fast atom bombardment (Kratos Mass Spectrometry 50; Kratos Analytical, Manchester, England). *N*-hydroxysulfosuccinimide and 1-ethyl-3-(3-dimethylaminopropyl) carbodiimide hydrochloride were purchased from Pierce Chemical in Rockford, Illinois. Most other chemicals were purchased from Aldrich Chemical in Milwaukee, Wisconsin. ^{18}F FDG was purchased from the Positron Diagnostic Research Center of the University of Texas. Silica gel–coated thin-layer chromatography plates were purchased from Whatman in Clifton, New Jersey.

Synthesis of Ethylenedicysteine

Ethylenedicysteine was prepared in a two-step synthesis process according to methods described by Blondeau et al (25) and Ratner and Clarke (26). Briefly, cysteine hydrochloride (41.52 g) was dissolved in 106 mL of water. Formaldehyde (26.1 mL) was added to the cysteine hydrochloride solution, and the reaction mixture was stirred overnight at room temperature. Pyridine (26.6 mL) was then added to the solution, and the precipitate formed. The crystals were separated and washed with 54 mL of ethanol for 25 minutes at room temperature and then filtered with a Buchner funnel (Alken-Murray, New Hyde Park, NY). The crystals were triturated with 150 mL of petroleum ether, filtered again, and then lyophilized for 3 days. The precursor, L-thiazolidine-4-carboxylic acid (melting point, 195°; reported 196°C to 197°C), was used for synthesis of ethylenedicysteine. The precursor (22 g) was dissolved in 200 mL of liquid ammonia and refluxed. Sodium metal was added until the agent had a permanent blue color. Ammonium chloride was added to the blue solution, and then the solvents were evaporated until they were dry. The residue was dissolved in 200 mL of water, and the pH was adjusted to 2. The precipitate that formed was filtered and washed with 500 mL of water. The solid material was dried in a calcium chloride vacuum dessicator (Aldrich Chemical, Milwaukee, Wis). Ethylenedicysteine was then prepared (melting point, 243°C to 246°C; reported 252°C to 253°C).

Synthesis of ECDG

Sodium hydroxide (concentration, 1 N; volume, 1 mL) was added to a stirred solution of ethylenedicysteine (concentration, 110 mg; volume, 0.41 mmol) in water (5 mL). To this colorless solution, *N*-hydroxysulfosuccinimide (concentration, 241.6 mg; volume, 1.12 mmol) and carbodiimide hydrocloride (concentration, 218.8 mg; volume, 1.15 mmol) were added. D-glucosamine hydrochloride salt (concentration, 356.8 mg; volume, 1.65 mmol) was then added. The solution was stirred at room temperature for 24 hours, and the pH was adjusted to 6.4–7.0. This solution was dialyzed for 48 hours by using a molecular porous membrane with a cutoff at 500 (Spectra/POR; Spectrum Medical Industries, Houston, Tex). After dialysis, the product was freeze dried with a lyophilizer (Labconco, Kansas City, Mo). The product weighed 291 mg (yield 60%). The product was depicted at proton nuclear MR imaging as follows: (D_2O) δ 2.60–2.90 (multiple signals, 4H and $-\underline{CH_2}$-SH of ethylenedicysteine), 2.95 (triple signals, 2H, glucosamine 5-$\underline{CH}$-CH_2OH), 3.20 (double signals, 4H, glucosamine 6-$\underline{CH_2}OH$), 3.30–3.95 (multiple signals, 6H glucosamine 1,3,4-$\underline{CH}$ and 4H $\underline{CH_2}$-SH of ethylenedicysteine), 3.30–3.66 (multiple signals, 4H, CH_2-$\underline{CH_2}$- of ethylenedicysteine), 4.15–4.30 (triple signals, 2H, NH-$\underline{CH}$-CO of ethylenedicysteine), 4.60 (double signals, 2H, glucosamine 2-$\underline{CH}$-NH_2), where δ is the chemical shift. The fast atom bombardment mass spectrometry molecular weight was 591 (parent ion M^+, 20).

Pertechnetate was obtained from Syncor Pharmaceutical in Houston, Texas. Radiosynthesis of ^{99m}Tc ECDG was achieved by means of adding the required amount of ECDG (80–100 mg) and tin (II) chloride (100 μg) to the pertechnetate. Radiochemical purity was assessed at radio–thin-layer chromatography (Bioscan, Washington, DC), with 1 mol/L of ammonium acetate plus methanol (4:1) as the eluant. High-performance liquid chromatography with a sodium iodide detector and ultraviolet detector (254 nm) was performed on a gel permeation column (Biosep SEC-S3000, 7.8 × 300 mm; Phenomenex, Torrance, Calif) at a flow rate of 1.0 mL/min. The eluant was 0.1% lithium bromide in

TABLE 1
Summary of Rodent Studies

Study	Total No. of Rodents
Glucose loading*	9
Group 1: rats injected with glucosamine	
Group 2: rats injected with ECDG	
Group 3: rats injected with ECDG plus 3 units of insulin	
Tissue distribution†	18
Group 1: injected with ^{99m}Tc ECDG	
Mice sacrificed at 0.5 h	
Mice sacrificed at 2.0 h	
Mice sacrificed at 4.0 h	
Group 2: injected with ^{18}F FDG	
Mice sacrificed at 0.5 h	
Mice sacrificed at 2.0 h	
Mice sacrificed at 4.0 h	
Gamma scintigraphy	21
Group 1: tumor volume vs ^{99m}Tc ECDG uptake‡	
In small tumors	
In medium tumors	
Group 2: ^{99m}Tc ECDG vs ^{99m}Tc EC uptake§	
^{90m}Tc EC	
^{99m}Tc ECDG	
Group 3: glucose-mediated uptake‖	
^{99m}Tc ECDG	
FDG plus ^{99m}Tc ECDG	
Insulin plus ^{99m}Tc ECDG	

Note.—EC = ethylenedicysteine.

* The following three groups consisted of three rats each.

† Groups 1 and 2 consisted of three mice each, which were sacrificed at 0.5 (n = 3), 2.0 (n = 3), and 4.0 (n = 3) hours after radionuclide administration.

‡ There were three rats each in the small and medium tumor groups.

§ Three rats were injected with ^{99m}Tc EC, and three rats were injected with ^{99m}Tc ECDG.

‖ Three rats were injected with ^{99m}Tc ECDG; three rats, with FDG plus ^{99m}Tc ECDG; and three rats, with insulin plus ^{99m}Tc ECDG.

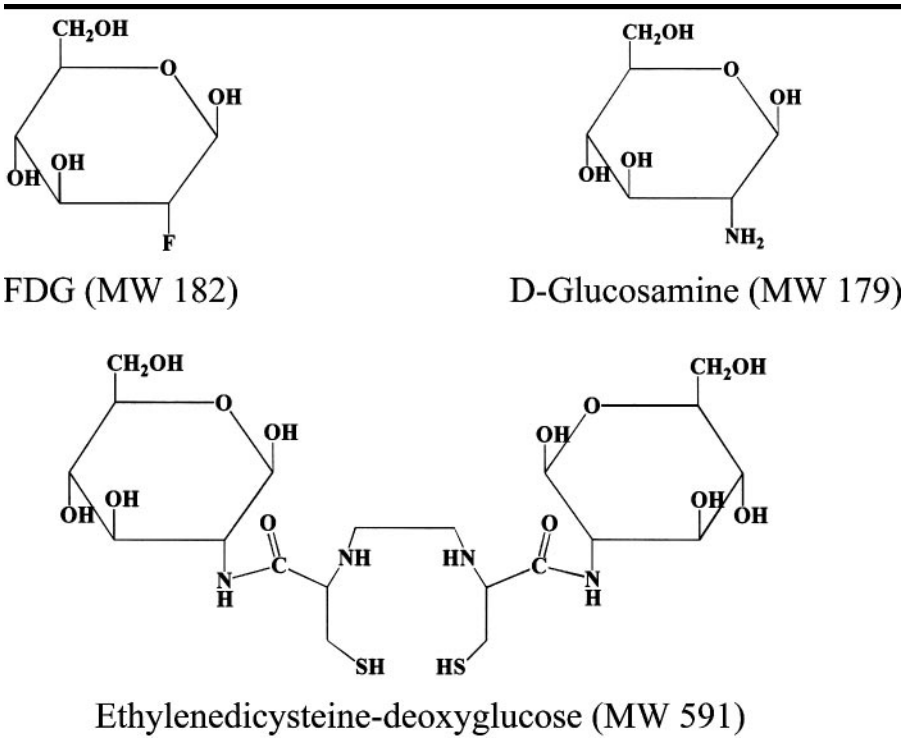

Figure 1. Synthesis of ^{99m}Tc ECDG: D-glucosamine is reacted with ethylenedicysteine in the presence of coupling agents, and tin (II) chloride and pertechnetate were added to the solution. *MW* = molecular weight.

phosphate-buffered saline (10 mmol/L, pH = 7.4).

Hexokinase Assay

To determine if ECDG mimics glucose phosphorylation (31), a hexokinase assay was performed. By using a ready-made assay kit (Sigma Chemical, St Louis, Mo), 1.0 mg of ECDG, 1.0 mg of FDG, and 1.0 mg of D-glucosamine each were dissolved in 1 mL of water separately, and 2.5 mg of D-glucose was dissolved in 2.5 mL of water. Next, 200 μL was removed from each of the four solutions and diluted in 2.5 mL of water. A 10-μL aliquot of each solution was removed, mixed with 900 μL of glucose reagent (Infinity Glucose Reagent; Sigma Chemical), and then incubated at 37°C for 3 minutes. The reduced-form of nicotinamide adenine dinucleotide was then assayed at an ultraviolet wavelength of 340 nm.

In Vitro Cellular Uptake Assay

In vitro cellular uptake assay was performed by using a human lung cancer cell line, A549. Each well (n = 12) that contained 80,000 cells was added to 0.074 MBq of ^{99m}Tc ECDG (in one group of six wells) and to 0.074 MBq of ^{18}F FDG (in another group of six wells). After the cells were incubated for 0.5–4.0 hours, we washed them with phosphate-buffered saline three times and then with trypsin one time to remove some of the cells with radiotracer uptake. To evaluate if the uptake of ^{99m}Tc ECDG in cells is mediated by means of a D-glucose mechanism, we added 1.0 mg of D-glucose, 2.0 mg of L-glucose, and 0.074 MBq of ^{99m}Tc ECDG to each well that contained lung cancer cells (50,000 cells per 0.5 mL of solution per well). After the cells were incubated for 2 hours, we washed them with phosphate-buffered saline three times and then with trypsin one time to remove some of the cells with radiotracer uptake. The cells were counted by a gamma counter (Packard Instrument, Downers Grove, Ill).

Effect of ECDG Loading on Blood Glucose Level

The animals were housed at The University of Texas M.D. Anderson Cancer Center. All protocols involving animals (eg, rats and mice) were approved by the M.D. Anderson Animal Use and Care Committee. To determine whether the blood glucose level could be increased by administering either glucosamine or ECDG and decreased by administering insulin, we deprived nine healthy Fischer 344 rats (Harlan, Indianapolis, Ind) (three rats per agent), which weighed 145–155 g, of food overnight prior to the experiments. The concentrations of prepared glucosamine hydrochloride and ECDG were 60% and 164% (milligram percentage), respectively. Blood glucose level (in milligrams per deciliter [SI: millimoles per liter]) was measured by using a glucose meter (Glucometer DEX; Bayer, Elkhart, Ind). The baseline blood glucose level was determined prior to the study. Each rat (n = 6) was injected with 1.2 mmol of glucosamine (group 1, n = 3) or

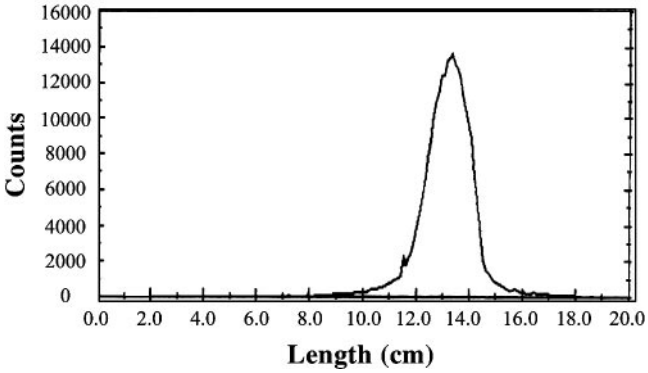

Figure 2. ECDG (98.7 mg) was labeled with 100 mCi (3,700 MBq) of $NaTcO_4$ in the presence of stannous chloride and spotted on an instant thin-layer chromatography strip. The eluant used was 1 mol/L of ammonium acetate with methanol (4:1). The radio–thin-layer chromatography data shown indicate 98.5% radiochemical purity. The data shown on the two axes represent counts of ^{99m}Tc ECDG and length of the eluant migrated.

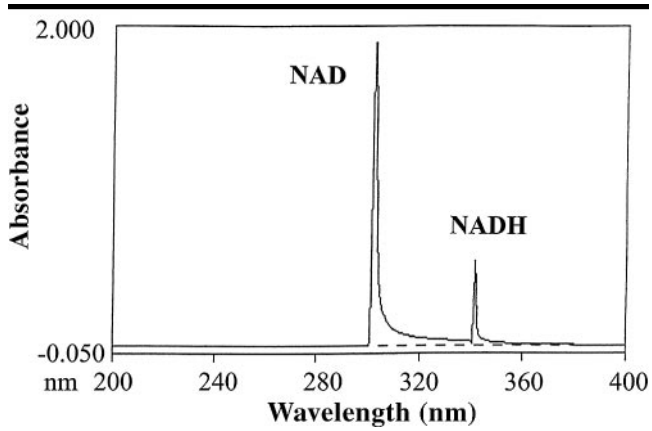

Figure 3. Graph depiction of the results of hexokinase assay performed to determine the phosphorylation of ECDG. ECDG phosphorylation was determined by means of coupling hexokinase activity with the reduction of nicotinamide adenine dinucleotide *(NAD)* to its reduced form *(NADH)*. The absorption of reduced-form nicotinamide adenine dinucleotide occurs at an ultraviolet wavelength of 340–350 nm; this indicates positive glucose phosphorylation activity (341.5 nm). The absorption of nonreduced nicotinamide adenine dinucleotide occurs at an ultraviolet wavelength of 302.5 nm.

ECDG (group 2, $n = 3$) per kilogram of body weight.

In a separate experiment, three rats (group 3) were injected with ECDG and then with insulin (3 units) 30 minutes later. Blood samples from the tail vein were collected (D.F.Y.) every 30 minutes up to 6 hours after agent administration. The total numbers of rats examined in each experiment are listed in Table 1.

Tissue Distribution Studies with ^{99m}Tc ECDG

One author (D.F.Y.) intramuscularly injected A549 human lung cancer cells (3×10^6 cells per mouse) into the middle dorsal region in a total of 18 female athymic nude mice (Ncr-nu/nu; National Cancer Institute, Bethesda, Md). After the tumors reached a size of 6 mm in diameter, two separate biodistribution studies with ^{99m}Tc ECDG (group 1) and ^{18}F FDG (group 2) were conducted. Each group of nine mice received ^{99m}Tc ECDG or ^{18}F FDG intravenously. The injection activity per mouse was 1–3 μCi (0.037–0.111 MBq) per mouse. The injected amount of ^{99m}Tc ECDG was 0.2 mg per mouse.

In both groups of nine mice each, the animals were divided into three groups: The animals in the first group were sacrificed 0.5 hour after radiotracer administration; those in the second group, 2 hours afterward; and those in the third group, 4 hours afterward. After the rodents were sacrificed, selected tissues were excised and weighed, and the radioactivity was measured. The biodistribution of radiotracer in each tissue sample was calculated as a percentage of the injected dose per gram of wet tissue weight. Tumor-to–nontargeted tissue ratios were calculated from the corresponding values of injected dose per gram of wet tissue weight.

Gamma Scintigraphy Studies

The animal model used was that of breast tumor–bearing rats, because their size is suitable for imaging. One author (D.F.Y.) inoculated female Fischer 344 rats that weighed 250–275 g with mammary tumor cells from the 13762 tumor cell line (subcutaneous, 10^6 cells per rat). This tumor cell line is specific to Fischer rats. After 8–10 days, tumor volumes of 0.3–0.6 cm were measured. Scintigrams were obtained 0.5, 2.0, and 4.0 hours after the intravenous injection of 300 μCi (11.1 MBq) of either ^{99m}Tc ethylenedicysteine (in three rats) or ^{99m}Tc ECDG (in three other rats). To demonstrate that different-sized tumors could be imaged, an author (D.F.Y.) performed imaging with ^{99m}Tc ECDG in two rat groups: three animals with small tumors and three with medium-sized tumors. We analyzed the whole-body images by defining regions of interest (ROIs, in counts per pixel), which were essentially outlines of particular organs. The ROI between tumor tissue and muscle (at an symmetric site) was used to determine tumor-to–nontumorous tissue ratios.

To ascertain whether tumor uptake of ^{99m}Tc ECDG was perfusion related, one author (A.A.) performed planar scintigraphy with ^{99m}Tc ethylenedicysteine and ^{99m}Tc ECDG in the breast tumor–bearing rats; 300 μCi (11.1 MBq) of the agent was intravenously administered to each rat.

To demonstrate that tumor uptake of ^{99m}Tc ECDG occurred by means of a glucose-mediated process, six tumor-bearing rats were pretreated with 200 mg/kg of saline (three rats) or 200 mg/kg of intravenously administered unlabeled FDG (three rats) and then injected with ^{99m}Tc ECDG (11.1 MBq) 30 minutes later. In a separate experiment, three rats were pretreated with 3 units of intramuscularly administered insulin and then injected with ^{99m}Tc ECDG 30 minutes later. The total numbers of rodents examined in each study are listed in Table 1. The tumor-to–nontumorous tissue ratios in the FDG–^{99m}Tc ECDG and insulin–^{99m}Tc ECDG groups were compared (by E.E.K.) with those in the ^{99m}Tc ECDG (control) group (three rats).

Scintigrams were obtained by using one of two imaging gamma cameras (Siemens M-camera, Siemens Medical Systems, Hoffman Estates, Ill; or 2020tc, Digirad, San Diego, Calif). Both cameras were equipped with a low-energy, parallel-hole collimator. The field of view with the Digirad camera is 20×20 cm with an edge of 1.3 cm. The intrinsic spatial resolution of the Digirad camera is 3 mm, and the matrix is 64×64. It is a solid-state gamma camera—that is, it does not have photomultiplier tubes—and is operated in a Windows NT (Microsoft, Redmond, Wash) format. With a preinstalled

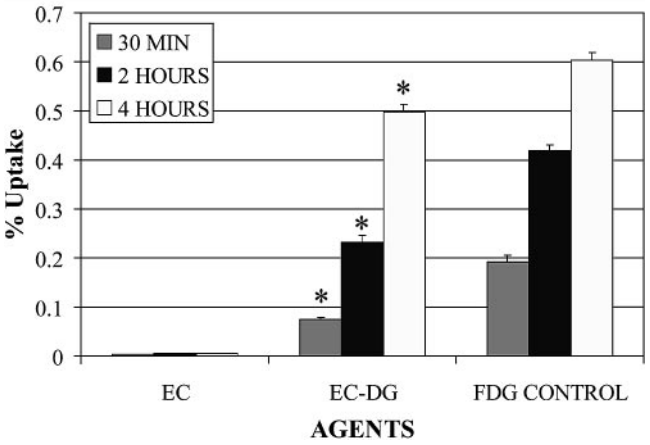

Figure 4. Bar graph illustrates the in vitro cellular uptake of ^{99m}Tc ECDG *(EC-DG)* and ^{18}F FDG. Graph data show that there was a markedly increased uptake of ^{99m}Tc ECDG and ^{18}F FDG as a function of time compared with the uptake of ^{99m}Tc ethylenedicysteine *(EC)*, the control agent. Asterisks indicate that there was a significant ($P < .05$, Student pair *t* test) difference between ^{99m}Tc ECDG uptake and ^{18}F FDG uptake during the same interval. Data are reported as means ± standard errors of the mean in the three agent groups. Data points were calculated as percentages of uptake.

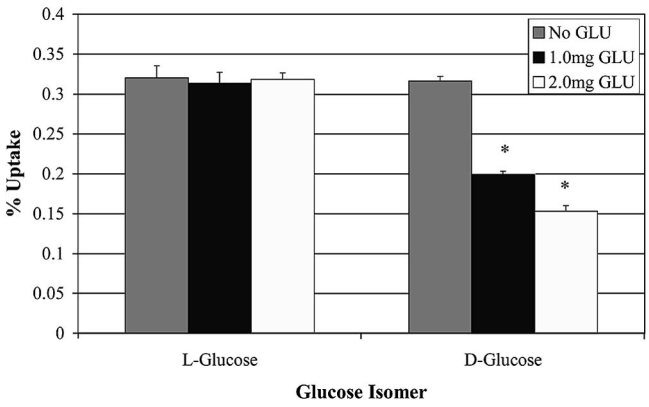

Figure 5. Bar graph illustrates the in vitro cellular uptake of ^{99m}Tc ECDG when glucose *(GLU)* was administered. Graph data show that there was a markedly decreased uptake of ^{99m}Tc ECDG as a function of D-glucose concentration compared with the uptake as a function of L-glucose concentration. Asterisks indicate that there was a significant ($P < .05$, Student pair *t* test) difference between the L-glucose– and D-glucose–loaded groups at equal concentrations. Data are reported as means ± standard errors of the mean in the three glucose dose groups. Data points were calculated as percentages of ^{99m}Tc ECDG uptake.

low-energy, high-spatial-resolution collimator (as is required for use with ^{99m}Tc), the system is designed to yield a planar sensitivity of at least 125 counts per minute per microcurie and a spatial resolution of 7.6 mm.

Statistical Analysis

The in vitro percentage of cellular uptake, in vivo percentage of injected dose per gram of wet tissue weight, and tumor-to–nontumorous tissue ratios are presented as means ± standard errors of the means. To compare differences in percentage of cellular uptake between the ^{99m}Tc ECDG and ^{18}F FDG groups and the difference between ^{99m}Tc ECDG uptake following the addition of D-glucose and that following the addition of L-glucose, the Student *t* test was used. $P < .05$ indicated a statistically significant difference. All statistical computations were processed by using a computer software program (Excel; Microsoft).

RESULTS

Chemistry

The chemical scheme of ^{99m}Tc ECDG synthesization is shown in Figure 1. ^{99m}Tc ECDG was determined at radio–thin-layer chromatography to have a radiochemical purity of 93.8%–100% (mean, 96.4%) (Fig 2). The yield of radioactivity is dependent on the physical amount of the agent used for radiolabeling. The amount of agent injected for high-performance liquid chromatography was 10 μCi (0.37 MBq)/10 μL/10 μg. The specific radioactivity was calculated to be 0.5 Ci/mmol (18.5 GBq/mmol).

Hexokinase Assay

A positive hexokinase assay result is characterized by a peak signal in the range of 340–350 nm. The results of hexokinase assay showed that ECDG could be phosphorylated (Fig 3). The findings suggested that hexokinase-catalyzed phosphorylation occurred with ECDG, deoxyglucose, FDG, and glucose. Whether ECDG and deoxyglucose use different glucose transporters needs to be further investigated.

In Vitro Cell Culture Studies

There was a marked increase in the uptake of ^{99m}Tc ECDG and ^{18}F FDG as a function of time compared with the uptake of ^{99m}Tc ethylenedicysteine. ^{99m}Tc ECDG had optimal uptake at 4 hours after injection and reached a level of 0.5% administered activity, whereas ^{18}F FDG had a greater than 0.6% uptake at 4 hours after injection (Fig 4). Adding glucose at a concentration of 1–2 mg per well led to a decreased uptake of ^{99m}Tc ECDG in lung cancer cells. However, L-glucose had no influence on ^{99m}Tc ECDG uptake (Fig 5). These findings suggest that the cellular uptake of ^{99m}Tc ECDG is mediated by way of a D-glucose mechanism.

Effect of D-Glucosamine and FDG Loading on Blood Glucose Level

The blood glucose level increased after the bolus intravenous administration of glucosamine in group 1 and of ECDG in group 2. This increased blood glucose level was suppressed by the administration of insulin in group C (Fig 6). The total number of rodents examined is shown in Table 1.

Tissue Distribution Studies

In group 1, ^{99m}Tc ECDG had higher tumor-to–muscle tissue and tumor-to–brain tissue ratios as a function of time, whereas in group 2, ^{18}F FDG had higher tumor-to-blood ratios. There were no significant differences in calculated tumor-to–lung tissue ratios (Tables 2 and 3).

Gamma Scintigraphy Studies

The smallest tumor volume that could be detected by using ^{99m}Tc ECDG was 3 mm. There was a significant increase in uptake, as demonstrated by the computer-generated ROI ratios of tumor versus nontumorous uptake as a function of time. The mean ROI ratios of ^{99m}Tc ECDG uptake determined immediately, 30 minutes, and 2 hours after radionuclide administration for the tumors versus the corresponding nontumorous regions (ie, in the opposite leg) were 1.70 ± 0.21, 1.58 ± 0.30, and 1.82 ± 0.07, respectively, for the small tumors and 2.36 ± 0.06, 2.41 ± 0.10, and 2.88 ± 0.10, respectively, for the medium-sized

tumors. The ranges of ROI counts for the tumor and nontumorous regions were 4,500–16,000 and 2,500–7,000, respectively. The pixel number was determined to be 213. The medium-sized (6-mm) tumors showed higher uptake at each time point. The heart, kidneys, liver, and bladder were visualized (Fig 7). Scintigrams demonstrated that breast tumors in rats could be better visualized with ^{99m}Tc ECDG scintigraphy than with ^{99m}Tc ethylenedicysteine scintigraphy at similar time points (Fig 8).

The rats pretreated with intravenously administered FDG (50 mg per rat) had decreased (40% at ROI analysis) tumor uptake of ^{99m}Tc ECDG. However, the rats pretreated with intramuscularly administered insulin (3 units) had increased (60% at ROI analysis) uptake of ^{99m}Tc ECDG 0.5–2.0 hours after agent administration. Selected scintigrams obtained 30 minutes after agent administration are shown in Figure 9.

TABLE 2
Biodistribution of ^{99m}Tc ECDG in Lung Tumor–Bearing Mice

Region of ^{99m}Tc ECDG Uptake	30 Minutes	2 Hours	4 Hours
Blood	1.607 ± 0.389	0.977 ± 0.267	0.787 ± 0.152
Lung	1.048 ± 0.259	0.721 ± 0.210	0.606 ± 0.128
Liver	5.674 ± 2.089	5.807 ± 1.708	6.656 ± 1.786
Stomach	0.540 ± 0.113	0.439 ± 0.138	0.541 ± 0.119
Spleen	3.240 ± 1.709	4.205 ± 1.374	5.933 ± 3.194
Kidney	6.726 ± 1.842	5.687 ± 1.540	4.318 ± 0.890
Thyroid	0.929 ± 0.212	0.665 ± 0.207	0.692 ± 0.119
Muscle	0.264 ± 0.072	0.148 ± 0.039	0.147 ± 0.022
Intestine	0.510 ± 0.093	0.417 ± 0.110	0.374 ± 0.073
Tumor	0.787 ± 0.163	0.415 ± 0.123	0.414 ± 0.161
Brain	0.058 ± 0.008	0.042 ± 0.006	0.042 ± 0.006
Heart	0.611 ± 0.193	0.336 ± 0.080	0.318 ± 0.071
Tumor-to–blood tissue ratio	0.499 ± 0.022	0.424 ± 0.022	0.502 ± 0.120
Tumor-to–muscle tissue ratio	3.352 ± 0.749	2.754 ± 0.120	2.795 ± 0.982
Tumor-to–lung tissue ratio	0.769 ± 0.047	0.587 ± 0.046	0.640 ± 0.120

Note.—All data are the mean percentage (for values obtained in three mice) of the injected dose of ^{99m}Tc ECDG per gram of wet tissue, ± the standard error of the mean, at 30 minutes, 1 hour, and 4 hours after administration of the agent.

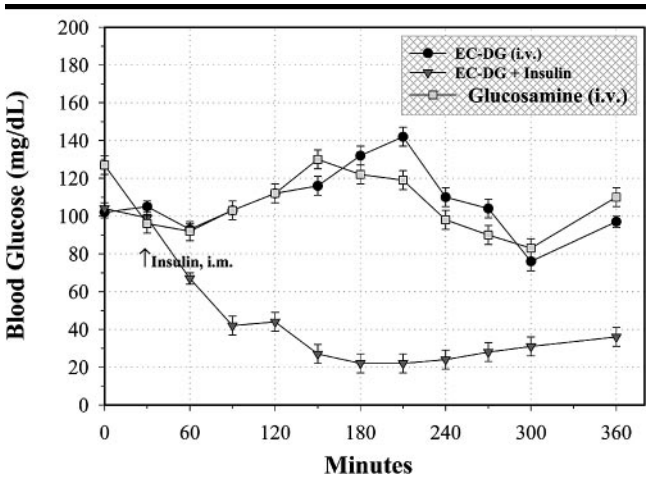

Figure 6. Data plotted to illustrate the intravenous *(i.v.)* administration of ECDG *(EC-DG)* and glucosamine in rats show increasing blood glucose levels as a function of time up to nearly 210 minutes after injection. Intravenous administration of ECDG and insulin caused a marked decrease in blood glucose levels.

DISCUSSION

The findings in the present studies appear to support our initial hypothesis that ^{99m}Tc ECDG has the potential to be used as a functional metabolic imaging agent. ^{99m}Tc ECDG is positive for phosphorylation at hexokinase assay on the basis of a peak signal in the range of 340–350 nm. This peak represents the ultraviolet absorbency of reduced-form nicotinamide adenine dinucleotide. Nicotinamide adenine dinucleotide, which is included in the hexokinase assay kit, changes to its reduced form during the phosphorylation of glucose in the mitochondria. Thus, we conclude that ECDG, the substrate, is phosphorylated by hexokinase, the enzyme, and that nicotinamide adenine dinucleotide changes to reduced-form nicotinamide adenine dinucleotide, which has a known ultraviolet absorbency that serves as an indicator of a positive assay result.

In addition, the uptake of ^{99m}Tc ECDG in lung tumor cell lines is comparable to that of ^{18}F FDG. Both agents accumulate owing to the increased metabolism (ie, increased need for glucose) in proliferating tumor cells. It has been reported that there are at least two mechanisms for the cellular processes of glucosamine (32,33). The first mechanism is similar to the cellular process mechanism of glucose: Glucosamine enters cells by way of a glucose transporter system, and then by way of phosphate and glycolytic pathways, and forms glucosamine-6-phosphate. In the second mechanism, glucosamine enters cells and directly forms glucosamine-6-phosphate. The regulatory products derived from glucosamine-6-phosphate are involved in translocation, transcription, and insulin action cascade. FDG is involved in the glucose phosphate and glycolytic pathways but not in the additional transcriptional pathways. Therefore, ^{99m}Tc ECDG may reflect more signaling biosynthetic pathways than ^{18}F FDG.

Overexpression of different glucose transporter types may lead to higher or lower detection specificity for radionuclides. ^{99m}Tc ECDG was superior to ^{18}F FDG with regard to tumor-to–brain tissue and tumor-to–muscle tissue ratios, whereas ^{18}F FDG had higher tumor-to-blood ratios. Lower tumor-to-blood ratios of ^{99m}Tc ECDG are owing to the higher concentration of this agent in blood compared with the concentration of ^{18}F FDG in blood. This higher concentration may result from the chemical modifications required to synthesize ^{99m}Tc ECDG, which can affect uptake kinetics and thus result in an increase in circulation time, flow to the kidneys, and excretion, all of which can also affect tumor uptake. ^{18}F FDG showed higher uptake in the tumor, brain, and heart than did ^{99m}Tc ECDG. The lower uptake of ^{99m}Tc ECDG by nor-

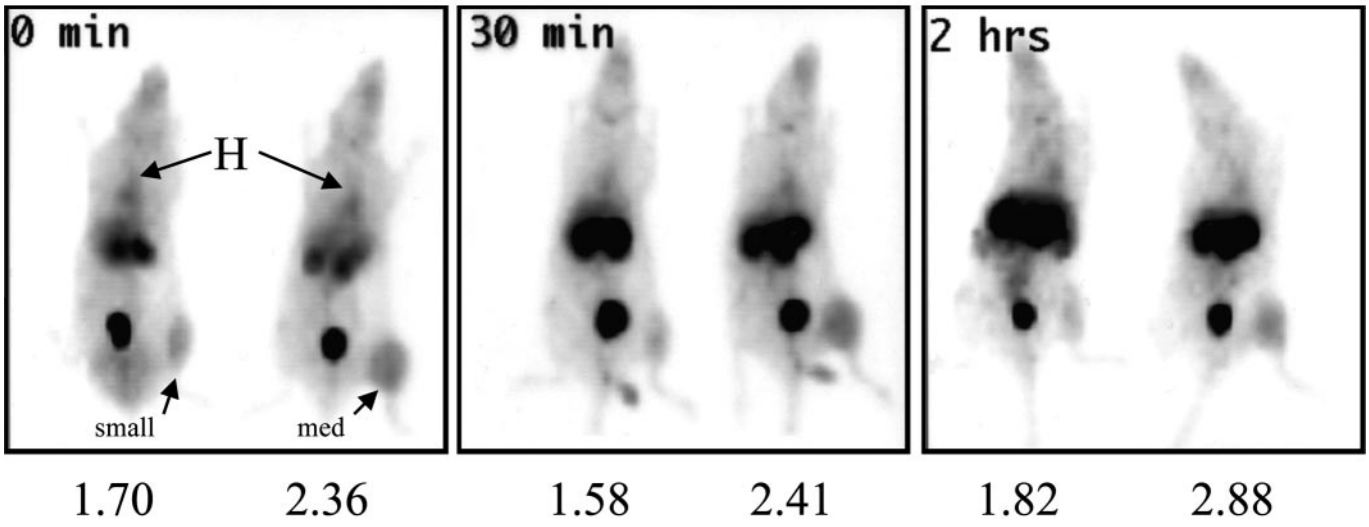

Figure 7. Planar scintigrams of ^{99m}Tc ECDG (300 μCi [11.1 MBq] per rat administered intravenously) uptake in breast tumor–bearing rats demonstrate that small (3-mm) and medium-sized (*med,* 6-mm) neoplasms could be imaged up to 2 hours after radionuclide administration. Arrows in the left image point to small and medium-sized tumors. The mean tumor-to-nontumor (opposite leg) ROI ratios determined immediately, 30 minutes, and 2 hours after ^{99m}Tc ECDG injection were 1.70 ± 0.21, 1.58 ± 0.30, and 1.82 ± 0.07, respectively, for the small tumors and 2.36 ± 0.06, 2.41 ± 0.10, and 2.88 ± 0.10, respectively, for the medium-sized tumors. Uptake was also observed in the heart *(H)*, liver, kidneys, and bladder.

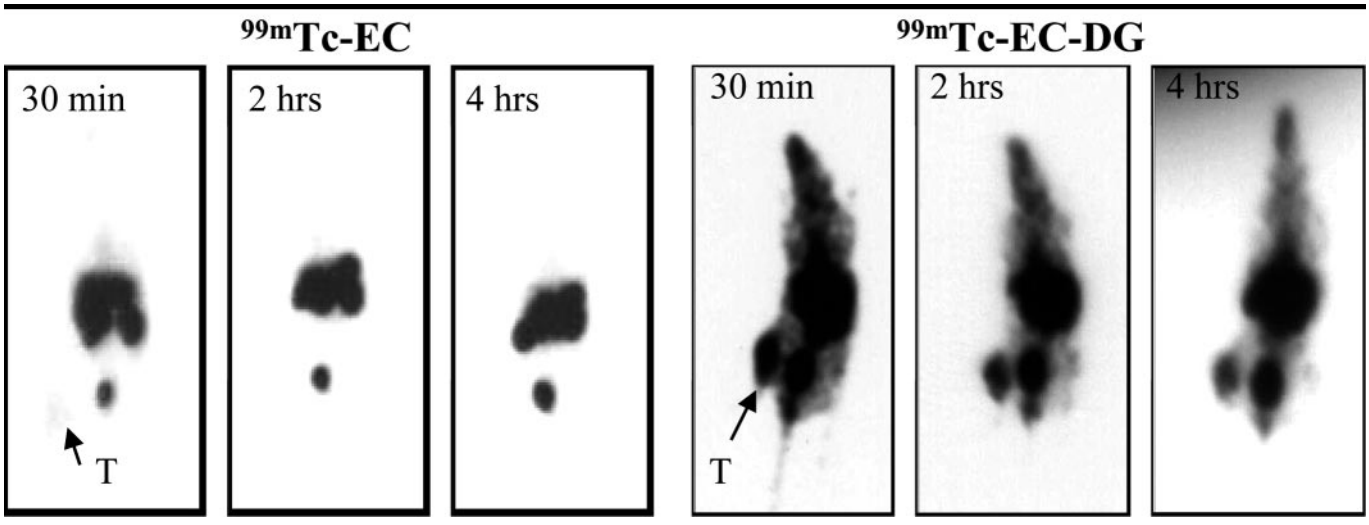

Figure 8. Planar scintigrams of ^{99m}Tc ethylenedicysteine *(^{99m}Tc-EC)* and ^{99m}Tc ECDG *(^{99m}Tc-EC-DG)* uptake in breast tumor–bearing rats (300 μCi [11.1 MBq] per rat administered intravenously) demonstrate that the tumor could be better imaged at ^{99m}Tc ECDG scintigraphy. Arrows point to tumors *(T)*.

mal brain tissue may have been due to coordination chemistry factors.

^{99m}Tc is stabilized by electrons from the nitrogen and sulfur components of ethylenedicysteine; hence, the charge of ^{99m}Tc may reduce uptake across the blood-brain barrier and in healthy brain cells. Therefore, brain tumors may be effectively detected with ^{99m}Tc ECDG imaging. ^{18}F FDG is a neutral molecule and can cross the blood-brain barrier easily compared with ^{99m}Tc ECDG. Thus, FDG PET may not be as effective in the diagnosis of low-grade brain tumors owing to high levels of ^{18}F FDG uptake in normal gray matter. Because of the high tumor-to-background count density ratios generated with ^{99m}Tc ECDG imaging, this examination may be more suitable and effective in the detection of low-grade brain tumors than FDG PET.

The principal hypoglycemic hormone is insulin, which is produced in the islets of Langerhans in the pancreas. Insulin, which is secreted in response to an increase in blood glucose level shortly after meals, increases glucose entry into muscle and fat tissues and promotes glycogen synthesis and storage in the liver (34,35). The net result of these actions is a net decrease in blood sugar level. Multiple rats were injected with ECDG or FDG, and, as expected, their blood sugar level increased. The administration of insulin with each agent led to a dramatic and similar decrease in blood sugar level in each animal, demonstrating that the two agents have similar uptake mechanisms. The response to insulin may be an important parameter for physicians to consider for patients with diabetes who are administered ^{99m}Tc ECDG for imaging. Insulin will lower their blood sugar levels after the administration of ^{99m}Tc ECDG and thus prevent hyperglycemia, and it

may allow a larger population of patients to participate in ^{99m}Tc ECDG imaging studies.

The feasibility of performing imaging with ^{99m}Tc ECDG was evaluated in mammary tumor–bearing rats with tumors in the hind leg. First, the agent was compared with ^{99m}Tc ethylenedicysteine and enabled good visualization of the tumors at 2 and 4 hours after injection. ^{99m}Tc ethylenedicysteine is a blood flow agent that has no detection specificity for any tissue or organ. ^{99m}Tc ethylenedicysteine was delivered to the liver and kidneys owing to high levels of blood flow through these organs; the agent remained in these regions mainly owing to interactions between ethylenedicysteine, acetylcysteine (in the kidneys), and glutathione (in the liver and kidneys), with the result of trapping of the ^{99m}Tc ethylenedicysteine molecule. Having established the effectiveness of ^{99m}Tc ECDG in targeting tumor cells, we performed another study to evaluate the usefulness of this agent in the detection of small (3-mm) and medium-sized (6-mm) tumors. The agent effectively enabled the detection of each size of tumor up to 2 hours after injection while remaining stable, as evidenced by the low uptake in the thyroid gland, which suggested in vivo stability. Finally, the rats pretreated with FDG and injected with ^{99m}Tc ECDG had decreased tumor uptake compared with the rats that were not pretreated. This finding indicates that ^{99m}Tc ECDG has an uptake mechanism similar to that of FDG—that is, the two agents have the same transporter types—and that the uptake of ^{99m}Tc ECDG is inhibited by the presence of FDG (competitive inhibition). As expected, the effects of insulin, mimicking those of normal glucose, resulted in increased ^{99m}Tc ECDG tumor uptake.

Practical application: There are similarities between the uptake of ^{99m}Tc ECDG and the uptake of ^{18}F FDG in tumors, and our findings support the potential use of ^{99m}Tc ECDG as a functional metabolic imaging agent. In addition, ethylenedicysteine can be labeled with ^{99m}Tc easily, efficiently, and with high radiochemical purity, stability, and cost effectiveness. With the complex mechanisms expressed in tumor tissue growth, the described ^{99m}Tc ethylenedicysteine and drug conjugate technique allows mechanism-specific imaging of cellular targets with use of ^{99m}Tc ECDG. This examination has the potential to improve the diagnosis before and prognosis, planning, and monitoring of cancer treatment.

TABLE 3
Biodistribution of ^{18}F FDG in Lung Tumor–Bearing Mice

Region of ^{18}F FDG Uptake	30 Minutes	2 Hours	4 Hours
Blood	0.793 ± 0.067	0.236 ± 0.009	0.203 ± 0.062
Lung	2.490 ± 0.209	2.222 ± 0.137	2.280 ± 0.182
Liver	1.051 ± 0.057	0.586 ± 0.040	0.785 ± 0.039
Stomach	5.046 ± 0.461	4.374 ± 0.864	2.278 ± 0.455
Spleen	1.824 ± 0.196	1.903 ± 0.144	1.591 ± 0.161
Kidney	1.137 ± 0.117	0.553 ± 0.104	0.568 ± 0.027
Thyroid	4.490 ± 0.526	4.617 ± 0.400	4.424 ± 0.442
Muscle	4.876 ± 0.621	5.409 ± 0.611	4.743 ± 0.610
Intestine	2.322 ± 0.542	2.764 ± 0.496	1.562 ± 0.342
Tumor	2.226 ± 0.150	1.699 ± 0.172	1.606 ± 0.182
Brain	6.557 ± 0.390	3.113 ± 0.132	2.065 ± 0.080
Heart	11.94 ± 2.571	20.33 ± 7.675	19.35 ± 8.286
Tumor-to–blood tissue ratio	2.821 ± 0.144	7.261 ± 1.007	8.932 ± 1.973
Tumor-to–muscle tissue ratio	0.463 ± 0.026	0.319 ± 0.031	0.346 ± 0.048
Tumor-to–lung tissue ratio	0.912 ± 0.119	0.775 ± 0.113	0.717 ± 0.106

Note.—All data are the mean percentage (for values obtained in three mice) of the injected dose of ^{18}F FDG per gram of wet tissue, ± the standard error of the mean, at 30 minutes, 1 hour, and 4 hours after administration of the agent.

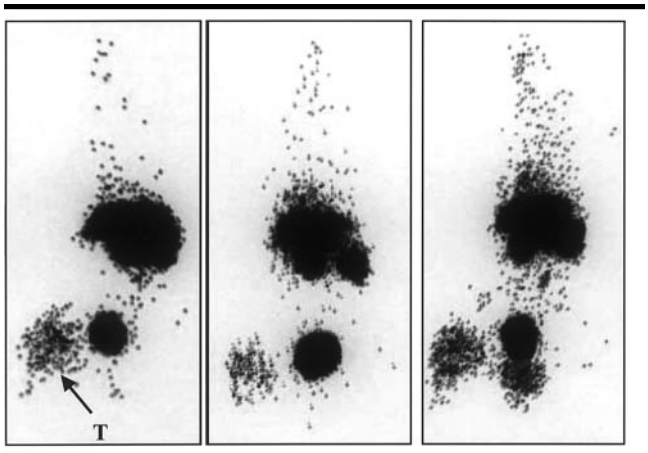

Figure 9. Planar scintigrams of ^{99m}Tc ECDG *(^{99m}Tc-EC-DG)* uptake (300 μCi [11.1 MBq] per rat administered intravenously) in breast tumor–bearing rats (three rats per agent group) obtained 30 minutes after injection demonstrate that pretreatment of the rats with FDG (middle image) or insulin (right image) affected the uptake of ^{99m}Tc ECDG. Arrow points to the tumor *(T)*.

Acknowledgment: The authors thank Eloise Daigle for her secretarial support.

References

1. Bar-Shalom R, Valdivia AY, Blaufox MD. PET imaging in oncology. Semin Nucl Med 2000; 30:150–185.
2. Plowman PN, Saunders CA, Maisey M. On the usefulness of brain PET scanning to the pediatric neuro-oncologist. Br J Neurosurg 1997; 11:525–532.
3. Weber WA, Avril N, Schwaiger M. Relevance of positron emission tomography (PET) in oncology. Strahlenther Onkl 1999; 175:356–373.
4. Lau CL, Harpole DH, Patz E. Staging techniques for lung cancer. Chest Surg Clin N Am 2000; 10:781–801.
5. Schulte M, Brecht-Krauss D, Heymer B, et al. Grading of tumors and tumor like lesions of bone: evaluation by FDG PET. J Nucl Med 2000; 41:1695–1701.
6. Yutani K, Shiba E, Kusuoka H, et al. Comparison of FDG-PET with MIBI-SPECT in the detection of breast cancer and axillary lymph node metastasis. J Comput Assist Tomogr 2000; 24:274–280.
7. Franzius C, Sciuk J, Daldrup-Link HE, Jurgens H, Schober O. FDG-PET for detection of osseous metastases from malignant primary bone tumors: comparison with bone scintigraphy. Eur J Nucl Med 2000; 27:1305–1311.
8. Folpe AL, Lyles RH, Sprouse JT, Conrad

EU, Eary JF. (F-18) fluorodeoxyglucose positron emission tomography as a predictor of pathologic grade and other prognostic variables in bone and soft tissue sarcoma. Clin Cancer Res 2000; 6:1279–1287.
9. Meyer PT, Spetzger U, Mueller HD, Zeggel T, Sabri O, Schreckenberger M. High F-18 FDG uptake in a low-grade supratentorial ganglioma: a positron emission tomography case report. Clin Nucl Med 2000; 25: 694–697.
10. Franzius C, Sciuk J, Brinkschmidt C, Jurgens H, Schober O. Evaluation of chemotherapy response in primary bone tumors with F-18 FDG positron emission tomography compared with histologically assessed tumor necrosis. Clin Nucl Med 2000; 25:874–881.
11. Carretta A, Landoni C, Melloni G, et al. 18-FDG positron emission tomography in the evaluation of malignant pleural diseases: a pilot study. Eur J Cardiothorac Surg 2000; 17:377–383.
12. Torre W, Garcia-Velloso MJ, Galbis J, Fernandez O, Richter J. FDG-PET detection of primary lung cancer in a patient with an isolated cerebral metastasis. J Cardiovasc Surg 2000; 41:503–505.
13. Brunelle F. Noninvasive diagnosis of brain tumors in children. Childs Nerv Syst 2000; 16:731–734.
14. Mankoff DA, Dehdashti F, Shields AF. Characterizing tumors using metabolic imaging: PET imaging of cellular proliferation and steroid receptors. Neoplasia 2000; 2:71–88.
15. Fitzgerald J, Parker JA, Danias PG. F-18 fluorodeoxyglucose SPECT for assessment of myocardial viability. J Nucl Cardiol 2000; 7:382–387.
16. Schwarz A, Kuwert T. Nuclear medicine diagnosis in diseases of the central nervous system. Radiology 2000; 40:858–862.
17. Roelcke U, Leenders KL. PET in neurooncology. J Cancer Res Clin Oncol 2001; 127:2–8.
18. Brock CS, Meikle SR, Price P. Does ^{18}F-fluorodeoxyglucose metabolic imaging of tumors benefit oncology? Eur J Nucl Med 1997; 24:691–705.
19. Ohtsuki K, Akashi K, Aoka Y, et al. Technetium-99m HYNIC-annexin V: a potential radiopharmaceutical for the in-vivo detection of apoptosis. Eur J Nucl Med 1999; 26:1251–1258.
20. Vriens PW, Blankenberg FG, Stoot JH, et al. The use of technetium ^{99m}Tc annexin V for in vivo imaging of apoptosis during cardiac allograft rejection. J Thorac Cardiovasc Surg 1998; 116:844–853.
21. Van Nerom CG, Bormans GM, De Roo MJ, Verbruggen AM. First experience in healthy volunteers with technetium-99m L,L-ethylenedicysteine, a new renal imaging agent. Eur J Nucl Med 1993; 20:738–746.
22. Canet EP, Casali C, Desenfant A, et al. Kinetic characterization of CMD-A2-Gd-DOTA as an intravascular contrast agent for myocardial perfusion measurement with MRI. Magn Reson Med 2000; 43: 403–409.
23. Laissy JP, Faraggi M, Lebtahi R, et al. Functional evaluation of normal and ischemic kidney by means of gadolinium-DOTA enhanced TurboFLASH MR imaging: a preliminary comparison with 99Tc-MAG3 dynamic scintigraphy. Magn Reson Imaging 1994; 12:413–419.
24. Kao CH, ChangLai SP, Chieng PU, et al. Technetium-99m methoxyisobutylisonitrile chest imaging of small cell lung carcinoma: relation to patient prognosis and chemotherapy response: a preliminary report. Cancer 1998; 83:64–68.
25. Blondeau P, Berse C, Gravel D. Dimerization of an intermediate during the sodium in liquid ammonia reduction of L-thiazolidine-4-carboxylic acid. Can J Chem 1967; 45:49–52.
26. Ratner S, Clarke HT. The action of formaldehyde upon cysteine. J Am Chem Soc 1937; 59:200–206.
27. Ilgan S, Yang DJ, Higuchi T, et al. ^{99m}Tc-ethylenedicysteine-folate: a new tumor imaging agent: synthesis, labeling and evaluation in animals. Cancer Biother Radiopharm 1998; 13:427–435.
28. Zareneyrizi F, Yang DJ, Oh CS, et al. Synthesis of ^{99m}Tc-ethylenedicysteine-colchicine for evaluation of antiangiogenic effects. Anticancer Drugs 1999; 10:685–692.
29. Yang DJ, Ilgan, S, Higuchi T, et al. Noninvasive assessment of tumor hypoxia with ^{99m}Tc-labeled metronidazole. Pharm Res 1999; 16:743–750.
30. Yang DJ, Azhdarinia A, Wu P, et al. In vivo and in vitro measurement of apoptosis in breast cancer cells using ^{99m}Tc-EC-annexin V. Cancer Biother Radiopharm 2001; 16:73–84.
31. Xie W, van de Werve G, Berteloot A. An integrated view of the kinetics of glucose and phosphate transport, and of glucose 6-phosphate transport and hydrolysis in intact rat liver microsomes. J Membr Biol 2001; 179:113–126.
32. Wells L, Vosseller K, Hart GW. Glycosylation of nucleocytoplasmic proteins: signal transduction and O-GlcNac. Science 2001; 291:2376–2378.
33. Marshall S, Bacote V, Traxinger RR. Discovery of a metabolic pathway mediating glucose-induced desensitization of the glucose transport system. J Biol Chem 1991; 266:4706–4712.
34. Gaudreault N, Santure M, Pitre M, Nadeau A, Marette A, Bachelard H. Effects of insulin on regional blood flow and glucose uptake in Wistar and Sprague-Dawley rats. Metabolism 2001; 50:65–73.
35. Fallavollita JA. Spatial heterogeneity in fasting and insulin-stimulated (18)F-2-deoxyglucose uptake in pigs with hibernating myocardium. Circulation 2000; 102: 908–914.